Mol Cell Biochem (2017) 428:57–66
DOI 10.1007/s11010-016-2916-6

Effect of poly-L-arginine in inhibiting scrapie prion protein of cultured cells

Muhammad Waqas[1] · Hye-Mi Lee[1] · Jeeyoung Kim[1] · Glenn Telling[2] · Jin-Ki Kim[1] · Dae-Hwan Kim[1] · Chongsuk Ryou[1]

Received: 12 October 2016 / Accepted: 21 December 2016 / Published online: 7 January 2017

Abstract Biological effect of poly-L-arginine (PLR), the linear homopolymer comprised of L-arginine, was investigated to determine the activity of suppressing prions. PLR decreased the level of scrapie prion protein (PrP^{Sc}) in cultured cells permanently infected with prions in a concentration-dependent manner. The PrP^{Sc} inhibition efficacy of PLR was greater than that of another prion-suppressant poly-L-lysine (PLK) in a molecular mass-dependent fashion. The effective concentration of PLR to inhibit prions was achieved safely below the cytotoxic concentrations, and overall cytotoxicity of PLR was similar to that of PLK. PLR did not alter the cellular prion protein (PrP^{C}) level and was unable to change the states of preformed recombinant PrP aggregates and PrP^{Sc} from prion-infected cells. These data eliminate the possibility that the action mechanism of PLR is through removal of PrP^{C} and pre-existing PrP^{Sc}. However, PLR formed complexes with plasminogen that stimulates prion propagation via conversion of PrP^{C} to the misfolded isoform, PrP^{Sc}. The plasminogen–PLR complex demonstrated the greater positive surface charge values than the similar complex with PLK, raising the possibility that PLR interferes with the role of cofactor for PrP^{Sc} generation better than PLK.

Keywords Poly-L-arginine · Prion · PrP^{C} · PrP^{Sc} · Inhibition

Introduction

Poly-L-arginine (PLR) is a linear homopolymer of basic amino acid L-arginine. The cationic property of PLR largely relies on the high pKa values of functional groups: 12.48 for L-arginine [1]. Due to such biochemical property, PLR is positively charged under physiological pH conditions. PLR has properties that mimic endogenous proteins, making them ideal for several biological applications, including delivery of chemical, nucleic acid, and peptide drugs both in vitro and in vivo [2–4]. In addition to its use as a vehicle, PLR itself has been used as surface material to adhere cells under in vitro conditions [5] and as an active agent to inhibit bacteria and viruses [6, 7]. Furthermore, PLR and the peptides that contain an oligoarginine stretch are effective to suppress tumor cell growth by stimulating immune responses [8, 9]. In fact, such an activity of PLR is induced through innate immune systems [10]. Prions are the causative agents of transmissible disorders in humans and animals, termed prion diseases [11, 12]. These diseases manifest progressive neuronal degeneration and subsequent death [11]. Currently, no therapy is available for prion diseases including Creutzfeldt–Jakob disease in humans [13, 14]. The prion agents are composed of the disease-causing, scrapie prion protein (PrP^{Sc}) only and propagate through macromolecular interaction between the normal, cellular prion protein (PrP^{C}) and PrP^{Sc} followed by conformational conversion of PrP^{C} to PrP^{Sc} [11].

Electronic supplementary material The online version of this article (doi:10.1007/s11010-016-2916-6) contains supplementary material, which is available to authorized users.

✉ Chongsuk Ryou
cryou2@hanyang.ac.kr

[1] Department of Pharmacy and Institute of Pharmaceutical Science and Technology, Hanyang University, 55 Hanyangdaehak-ro, Sangnok-gu, Ansan, Gyeonggi-do 15588, Republic of Korea

[2] Department of Microbiology, Immunology and Pathology, Colorado State University, Fort Collins, CO, USA

Recently, Mays and Ryou demonstrated that plasminogen assists in prion propagation facilitated by aforementioned protein conformation conversion process [15, 16]. Ryou et al. showed that plasminogen-assisted prion propagation is suppressed by poly-L-lysine (PLK) in vitro and in vivo [17]. Jackson et al. confirmed anti-prion activity of both stereo isomers of polylysine and showed that prion inhibition of polylysine is mediated by their complex formation with plasminogen [18]. PLR and PLK share similarities in structure and biochemical properties [19]. They have a linear amino acid backbone maintained by peptide bonds. PLR and PLK are cationic at the physiological pH because both are composed of basic amino acids [19, 20]. However, PLR differs from PLK by containing guanidinium functional groups instead of amine groups. Unlike PLK, anti-prion activity of PLR has not been investigated and its potency is not estimated. Discovery of anti-prion agents and expanded investigation are regarded important because, although rare, prion diseases pose a potential risk to public health. Here, we report the efficacy of PLR to inhibit prions in vitro. In particular, comparative analyses of PLR and PLK were performed regarding cytotoxicity and the properties to suppress PrP^{Sc} from multiple cell lines infected by prions. We also attempted to investigate how PLR exerts anti-prion effect by studying its effect on PrP^{C} levels, destabilization of preformed PrP aggregates and PrP^{Sc}, and complex formation with a previously proposed cofactor.

Materials and methods

Polymers, proteins, and chemical reagents

PLR and PLK used for this study are summarized in Table S1, in which the average molecular weights and the number of monomer units per polymer molecule are demonstrated. The average molecular weights of the polymers in KDa are used to designate different PLRs and PLKs. Both PLR38.5 and PLK33 purchased from Alamanda Polymers Inc (Huntsville, AL) are composed of the same number of monomer units. PLR10, PLR110, and PLK10 were purchased from Sigma-Aldrich (St. Louise, MO). The cell culture reagents, high glucose Dulbecco's modified Eagle's medium (DMEM), fetal bovine serum (FBS), penicillin-streptomycin, and Glutamax, were purchased from Invitrogen (Carlsbad, CA). Tris-HCl, sodium chloride, Nonidet P-40 (NP-40), sodium deoxycholate (DOC), 3-(4,5-dimethyl-2-thiazolyl)-2,5-diphenyl-2H-tetrazolium bromide (MTT) at the molecular biology grade, and thioflavine T (ThT) were purchased from Sigma-Aldrich. Proteinase K (PK) was purchased from Invitrogen. Silver stain kit, bicinchoninic acid protein assay kit, and peroxidase-conjugated secondary antibody used for this study were purchased from Pierce (Rockford, IL). Monoclonal anti-PrP antibody clone 5C6 [21], which recognizes the discontinuous epitope created by the residues 132 and 158, was kindly gifted from G. Telling, Colorado State University. Anti-PrP antibody 6D11, of which epitope spans the PrP residues 93–109, and SAF32, of which epitope locates at the PrP residues 57–88, were purchased from Covance (Dedham, MA) and Cayman Chemicals (Ann Arbor, MI), respectively. Anti-β-actin and anti-βIII tubulin antibodies were purchased from R&D System (Minneapolis, MN). ECL Prime Detection Reagents were purchased from Amersham (GE Healthcare, Piscataway, NJ). Other conventional chemicals and reagents at their finest grades were purchased from Sigma-Aldrich. Plasminogen purified from human sources (Glu-palsminogen) was purchased from Hematologic Technologies, Inc (Essex Junction, VT). Recombinant PrP was expressed and purified as described previously [22]. Briefly, the mouse PrP cDNA fragment spanning from the 89th to 231st amino acid residues was used to express as a His-tag fusion protein in E. coli, and this recombinant PrP, designated MoPrP(89–231), was purified using His-tag affinity chromatography.

Cell culture and treatment

Scrapie-infected Neuro-2a (ScN2a) cell line permanently infected by RML scrapie prions [23], SMB (scrapie mouse brain) cell line established from brains of mice infected by 139A scrapie prion strain [24], Elk21+ cell line established by permanent infection of RK13 (rabbit kidney 13) cells overexpressing cervid PrP with elk prions [25], and N2a neuroblastoma cell line free of prions were used in this study. Cell culture and treatment with polymers were performed according to the method described previously [17, 18]. Cells were initially seeded at 2% confluency in culture dishes (100-mm in diameter) and cultured with DMEM containing 10% FBS, 1% penicillin-streptomycin, and 1% Glutamax. Cells were incubated at 37 °C under 5% CO2 and saturated humidity conditions. As seeded cells were anchored onto the surface of culture containers, polymers of various concentrations were directly added to culture media. Incubation lasted for 6 days with a media replacement at the fourth day using fresh culture media containing polymers.

Detection of PrP^{Sc} and PrP^{C}

PrP^{Sc} assay was performed as previously described [17, 18]. Lysate of prion-infected cells incubated with polymers in the100-mm-diameter culture dishes was prepared in 1 ml cell lysis buffer (20mM Tris, pH 8.0; 150 mM NaCl; 0.5% NP-40; 0.5% DOC). For protein quantification

of cell lysate, bicinchoninic acid protein assay was performed as recommended by the manufacturer. 2 mg of cell lysate was incubated with 20 μg/ml PK for 1 h at 37 °C and subsequently centrifuged for 1 h at 16,000×*g* at 4 °C. PK-resistant PrP^{Sc} included in the pellet was detected by western blotting using anti-PrP antibody clone 5C6. Separately, an aliquot (~30 μg) of ScN2a or N2a cell lysate was analyzed without PK digestion by western blotting for total PrP using anti-[14] PrP antibody clones SAF32, 6D11, and 5C6. β-actin and βIII tubulin were also detected as the loading control. For PrP^{C} detection, ScN2a and N2a cell lysate were separated into the pellet, which includes insoluble PrP species-like PrP^{Sc}, and the supernatant, which includes soluble PrP species-like PrP^{C}, by ultracentrifugation for 1 h at 100,000×*g* at 4 °C. The supernatant (~20 μg) was used for western blotting to determine the level of PrP^{C} by anti-PrP antibody SAF32. PrP bands were detected with ECL Prime Detection Reagents using G:Box Chemi XR5 system and GeneTools software (Syngene, Cambridge, UK).

Cytotoxicity assay

The cytotoxicity of polymers was measured using the MTT assay protocol described previously [17, 18]. Briefly, ScN2a cells were plated in a 24-well culture container and incubated for 6 days with polymers to be tested. The cells were incubated for additional 2 h with DMEM containing 0.5 mg/ml MTT. Purple MTT formazan products extracted in 0.05 N HCl-isopropanol were quantified by colorimetric readouts at 570 nm with background subtraction at 650 nm using Infinite M200Pro Multimode Reader (Tecan, Männedorf, Switzerland).

PrP stability assay

PrP aggregate formation assay (PAFA) was employed to generate preformed PrP aggregates and was performed as described previously [26]. Briefly, MoPrP(89–231) at the final concentration of 50 μg /ml in 0.2 ml reaction buffer (phosphate buffered saline, pH 7.2, 0.4 M guanidine hydrochloride, 10 μM ThT) was incubated at 37 °C for 10–48 h with agitation at 300 rpm. The reactions were carried out in 96-well microplates from which fluorescence was detected in situ by Infinite M200Pro Multimode Reader (Tecan). Aggregates of MoPrP(89–231) generated by PAFA were saved at 4 °C until used for PrP stability assay. Preformed MoPrP(89–231) aggregates were equally aliquoted, mixed with 1 μM PLR10 or PLK10, and incubated for 36 h with occasional agitation at 300 rpm. Fluorescence of thioflavin T bound to PrP aggregates was measured by Infinite M200Pro Multimode Reader during incubation.

PrP^{Sc} of ScN2a cells was subjected to an independent assay to analyze its stability in the presence of polymers under different pH conditions. The assay was performed as described in our previous publications with minor modifications [18, 27]. Approximately 350 μg of ScN2a cell lysate was diluted in 0.6 ml reaction buffer (50 mM sodium acetate, 1% NP-40) at pH 4, 5, 6, and 7, and incubated with PLR38.5 at the final concentration of 1 μg/ml at 37 °C for 3 h with continuous agitation at 300 rpm. After pH neutralized, the reaction underwent PK digestion as described above in the PrP^{Sc} assay section. The PK-resistant material was recovered by methanol–chloroform precipitation [28] and analyzed by Western blotting. Control assay was also performed in the identical manner but without PLR.

Gel electrophoretic migration retardation assay

Polymer–plasminogen complex formation was assessed by the method described previously with minor modifications [18]. Plasminogen (0.25 μM, final concentration) was mixed with PLR38.5 and PLK33 (0.25–25 μM, final concentration) in 20 μl of 10 mM Tris buffer (pH 7.5) containing 5% glycerol (v/v) and incubated for 30 min at room temperature. The complex was analyzed by non-denaturing polyacrylamide gel electrophoresis. The mobility retardation of the complexes in the gel was visualized by silver staining according to manufacturer's instruction.

Measurement of particle size and surface charge

The formation of particles composed of polymer and plasminogen was achieved by the similar manner described above. Briefly, PLR and PLK were individually mixed with plasminogen (180 μg) in 1 ml of 10 mM Tris buffer (pH 7.5). The mean particle size and the surface charge (zeta potential) of the complexes were determined with a Zetasizer Nano ZS (Malvern, Worcestershire, UK) using dynamic light scattering (DLS) and electrophoretic light scattering (ELS), respectively [29]. The DLS analysis was performed with He–Ne laser (633 nm) at scattering angle of 173° at 25 °C. In ELS analysis, the complexes were loaded into a pre-rinsed folded capillary cell and the velocity of the complexes in an applied electric field of a known value was automatically interpreted by the method of Smoluchowski. All measurements were carried out in triplicate for each sample.

Results

PLR is more potent than PLK in inhibiting prions of ScN2a cells

To determine the efficacy of PLR in suppressing prions with respect to PLK, two separate groups of cultured

ScN2a cells were incubated each with PLR38.5 and PLK33, both of which contain the same number of monomer units (200-mers). Although both PLR and PLK demonstrated inhibitory effects to prions, PLR38.5 was more potent than PLK33 (Fig. 1a). In the cells incubated with PLR and PLK, PK-resistant PrP^{Sc} was removed in a concentration-dependent manner. Western blots showed that the complete elimination of PrP^{Sc} from the cells was accomplished with ~10 nM PLR38.5, while the substantial level of PrP^{Sc} remained in the cells incubated with the similar concentrations of PLK33. Next, anti-prion activity of PLR10 and PLK10 was compared to confirm the aforementioned observation that PLR is more potent than PLK. Although both required the higher concentrations than PLR and PLK with high polymerization degrees, PLR10 was more effective in inhibiting PrP^{Sc} propagation than PLK10 (Fig. 1b). These data indicate that PLR is more effective in interfering with prion propagation within cell populations.

Prion inhibition activity correlates with the molecular weights of PLR

Anti-prion activity of PLR polymers with different polymerization degrees, PLR10 (52-mers), PLR38.5 (200-mers), and PLR110 (571-mers) (Table S1), was compared to examine whether the molecular weight of polymers correlates with the enhancement of PrP^{Sc} inhibition activity. PrP^{Sc} of ScN2a cells was efficiently eliminated by PLR110 at the low nM concentrations (Fig. 1c). Compared to PLR10 and PLR38.5 (Fig. 1a, b), PLR110 was more potent for anti-prion activity. These data indicate that PLR polymers with the greater molecular weight are more effective in decreasing the level of PrP^{Sc}, showing that the potency of PLR is greater in order of PLR110, PLR38.5, and PLR10. The results shown (Fig. 1). are reminiscent of the data demonstrated in our previous studies, in which the efficacy of PLK to inhibit prion propagation is dependent on the concentrations and molecular weights of polymers [17].

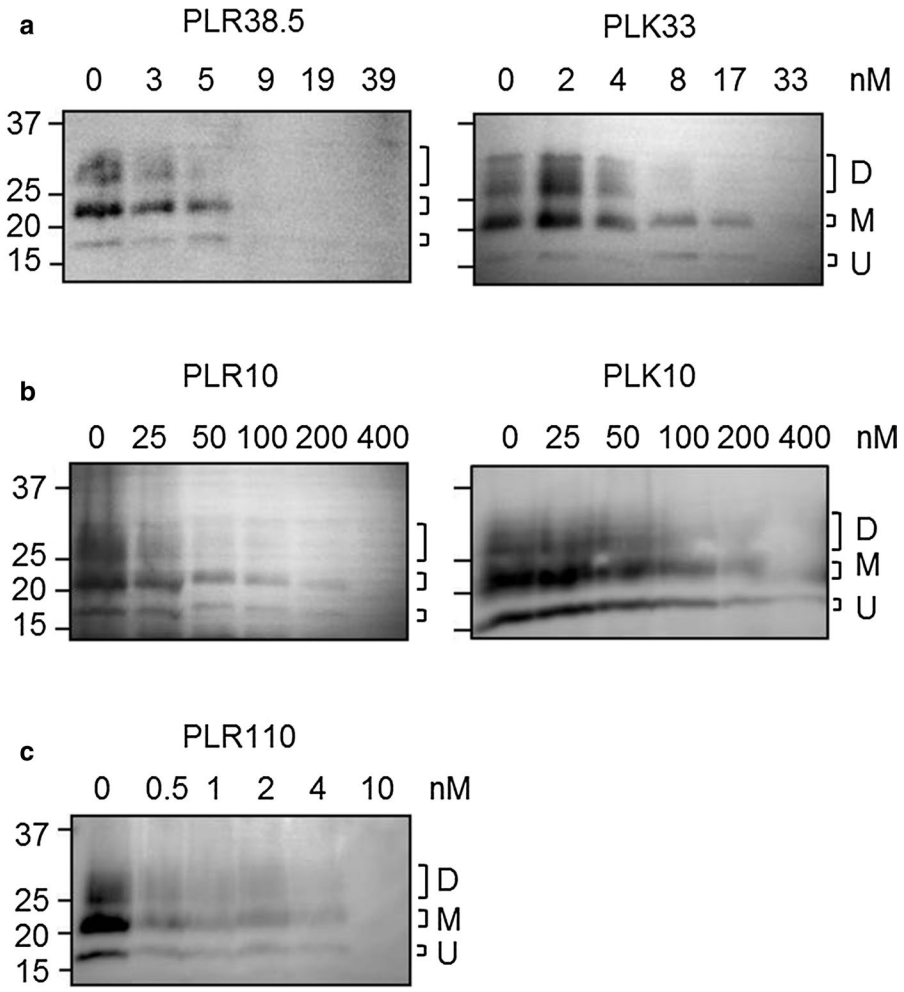

Fig. 1 Comparison of prion inhibition by PLRs and PLKs in ScN2a cells. Representative western blot analyses of PK-resistant PrP^{Sc} in ScN2a cells incubated with PLR38.5 and PLK33, (**a**) with PLR10 and PLK10 (**b**), and with PLR110 (**c**). Independent western blotting analyses were repeated ($n = 2$–4). In every replicate for each compound, the trend of dose-dependency for anti-prion effect was identical. Different glycoforms of PK-resistant PrP^{Sc} were marked with brackets. *D* diglycosylated, *M* monoglycosylated, *U* unglycosylated

Cytotoxicity of PLRs and PLKs is identical

To determine cytotoxicity of PLR, ScN2a cells were incubated with various concentrations of polymers. The cells survived under 0.1 μM, but completely died over 1 μM of PLR38.5 (Fig. 2a). The cytotoxicity profile of PLR38.5 was almost identical to that of PLK33. Similarly, both PLR10 and PLK10 shared the same pattern of cytotoxicity profile, demonstrating no induction of cytotoxicity under 1 μM, the highest concentration examined in this study for both polymers (Fig. 2b). These data suggest that cytotoxicity of PLRs and PLKs with the comparable polymerization degrees is not different. When cytotoxicity of PLR with different molecular weights was compared, the cells did not survive at 0.3 μM of PLR110 and at 1 μM of PLR38.5, while cell survival was obvious at 1 μM of PLR10 (Fig. 2c). Analogous to anti-prion activity of PLRs, this indicates that cytotoxicity was increased proportionally to the concentration and molecular weight of PLRs. Taken together with anti-prion efficacy tests, cytotoxicity study demonstrates that effective concentrations to eliminate PrP^{Sc} below the detection level are substantially lower than the cytotoxic concentrations, suggesting that anti-prion effect of PLR is not owing to the death of prion-infected cells.

PLR inhibits prions of multiple cell lines

Anti-prion activity of PLR in cell lines infected by prion strains other than RML was investigated using the same approaches. Incubation of SMB cells infected by the scrapie prion strain 139 A with the increasing concentrations of PLR38.5 resulted in efficient disappearance of PrP^{Sc} (Fig. 3a). Similarly, PrP^{Sc} of Elk21+ cell infected by cervid prions was efficiently removed by PLR38.5 (Fig. 3b). These results demonstrate that PLR is effective to inhibit PrP^{Sc} of multiple cell lines permanently infected with different prions.

The level of PrP^{C} is unaltered in cells incubated with PLR

The level of βIII tubulin or β-actin, the housekeeping gene product, was unaltered in ScN2a cells, although the cells were incubated with increasing concentrations of various PLRs (Figs. S1, 4). More interestingly, the level of PrP^{C} was not changed either, as judged by the bands, which migrated at ~25–37 KDa in western blots when detected with anti-PrP antibody clones 6D11 and 5C6 that recognize the epitopes at 93rd–109th and 132nd–158th amino acid

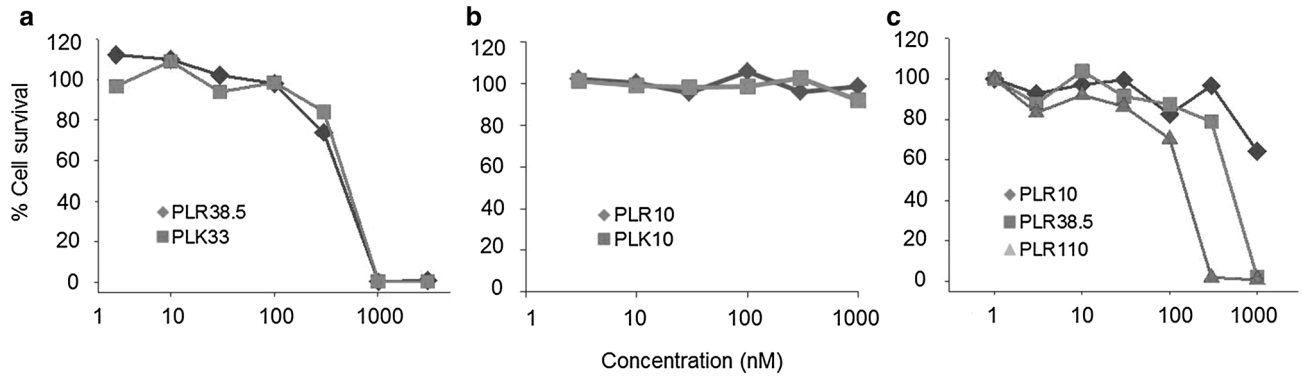

Fig. 2 Comparison of cytotoxicity between PLRs and PLKs. The results of MTT assay with PLR38.5 and PLK33 (**a**), PLR10 and PLK10 (**b**), and PLR10, PLR38.5, and PLR110 (**c**). The measurement was performed with duplicate samples from three independent assays

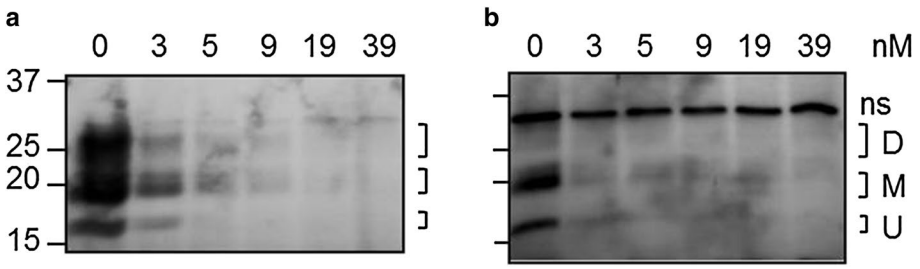

Fig. 3 Western blots of PK-resistant PrP^{Sc} in SMB (**a**) and Elk21+ (**b**) cells treated with various concentrations of PLR38.5. *ns* the non-specific signal detected in the Immunoblotting procedure. Different glycoforms of PK-resistant PrP^{Sc} were marked with brackets. *D* diglycosylated, *M* monoglycosylated, *U* unglycosylated

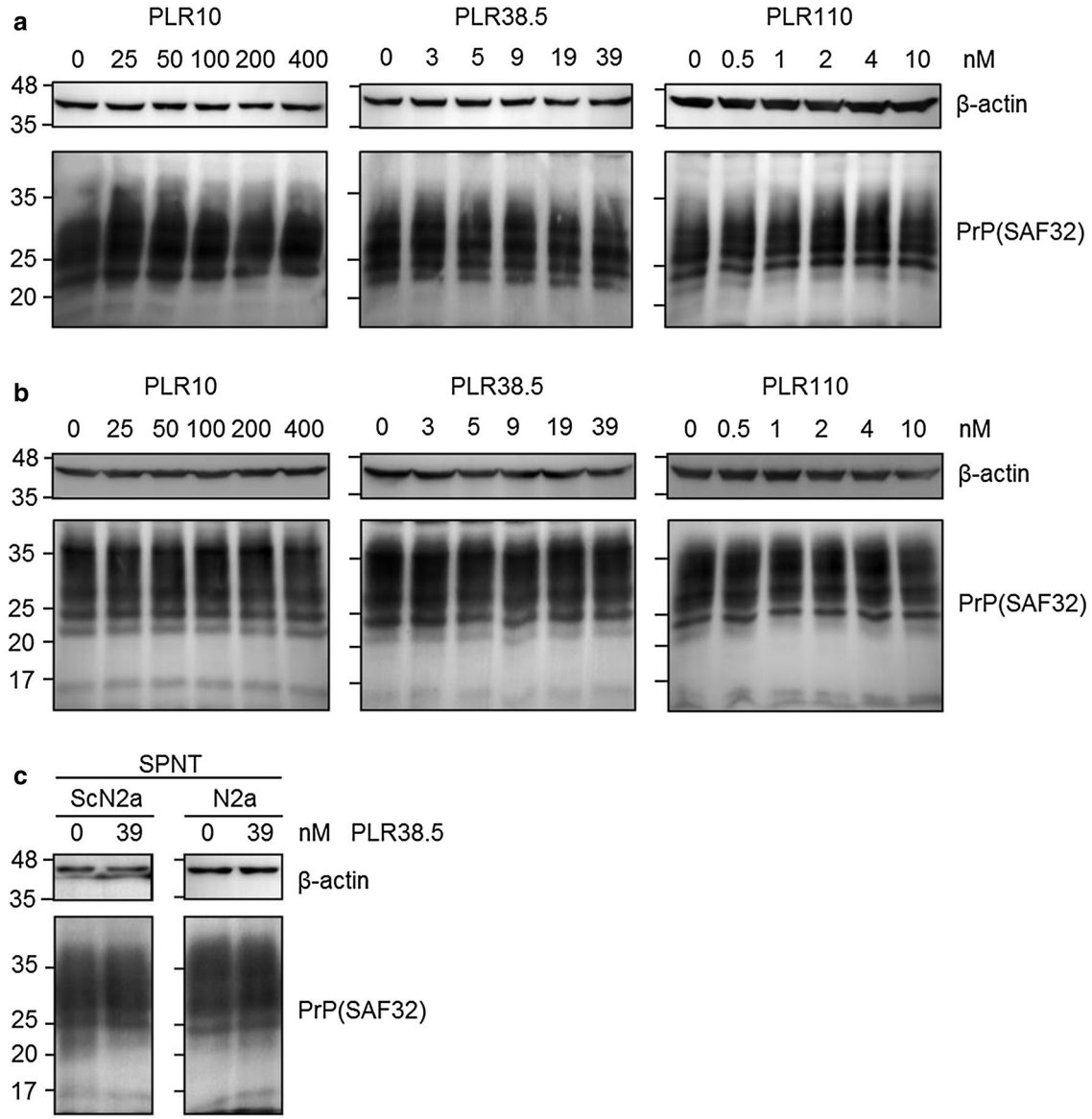

Fig. 4 The effect of PLR to the level of PrP^C. Detection of PrP in ScN2a (**a**) and N2a (**b**) cells incubated with various concentrations of PLR10, PLR38.5, and PLR110 was performed by immunoblotting with anti-PrP antibody SAF32, of which epitope locates at 57th–88th residues. Western blots of β-actin were shown with corresponding samples for PrP detection. **c** Detection of PrP^C solubilized in the supernatant (SPNT) of PLR- and mock-treated ScN2a and N2a cell lysates after exclusion of insoluble PrP^{Sc} by ultracentrifugation

residues of PrP, respectively (Fig. S1a). Similar to what was demonstrated in western blots of PK-digested samples, the bands seemingly originated from PrP^{Sc} molecules disappeared according to the increase of PLR concentrations in western blots of undigested samples representing total PrP molecules (Fig. S1a). No change of PrP^C level was further confirmed in western blots with anti-PrP antibody clones SAF32, which recognizes further N-terminal of PrP^C at 57th-88th residues (Fig. 4a).

Nonetheless, detection of PrP^C from ScN2a cell lysate is considered ambiguous because what was detected is total PrP, which includes both PrP^C and PrP^{Sc}. Thus, the effect of PLR to PrP^C was determined using N2a cells, the prion-free counterparts of ScN2a cells. The level of PrP^C was not changed in N2a cells incubated with different concentrations of PLRs when detected with anti-PrP antibody clones SAF32 and 6D11 (Figs. 1b, 4b). Furthermore, the level of PrP^C was comparable in the soluble, ultracentrifugal supernatant of both ScN2a and N2a cell lysates independent of incubation with PLR (Fig. 4c). These results suggest that inhibition of PrP^{Sc} propagation by PLR is not attributed to altered equilibrium of the PrP^C level.

PLR does not affect aggregated states and does not drive destabilization of preformed, misfolded PrP molecules

To determine whether PLR is able to dissociate preformed aggregates of recombinant PrP, the in vitro PAFA products were incubated with PLR10 and measured disappearance of ThT fluorescence representing the aggregated state of recombinant PrP. Compared to control reactions with vehicle, the reaction with PLR demonstrated no significant alteration of the aggregated PrP levels (Fig. 5a). We also investigated whether PLR induces destabilization of PrP^{Sc} at acidic pHs as demonstrated in previous studies using polyamine dendrimers [30, 31]. Incubation of PrP^{Sc} included in ScN2a cell lysate with PLR38.5 at acidic to neutral pHs resulted in no PLR-mediated destabilization of PrP^{Sc}, although acidic pH per se affected stability of PrP^{Sc} so that it became more vulnerable to be digested by PK (Fig. 5b). These results support that anti-prion activity of PLR is irrelevant to degradation or destabilization of preformed PrP aggregates or PrP^{Sc}. Such a characteristic of PLR resembles that of PLK [18], but differ from the activity of polyamine dendrimers that dissolve preformed PrP^{Sc} aggregates [30, 31].

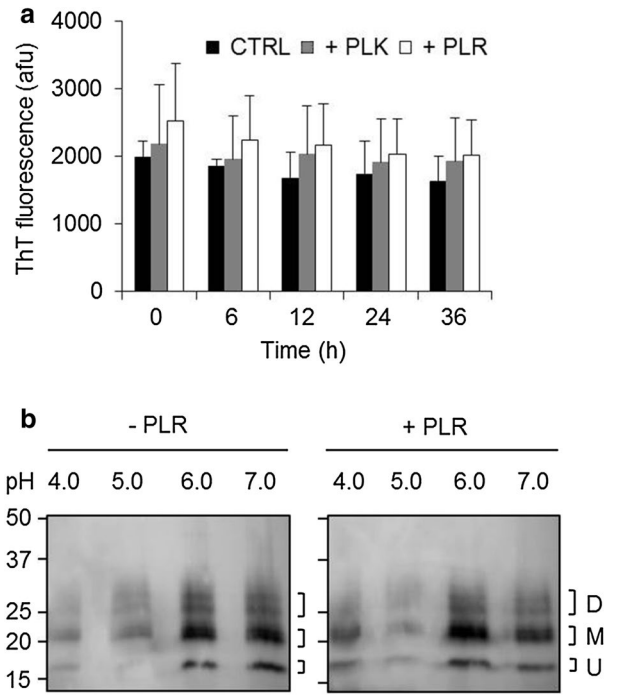

Fig. 5 Effect of PLR and PLK on stability of aggregated, misfolded PrP molecules. **a** ThT fluorescence measurement for preformed aggregates of recombinant mouse PrP incubated with PLR10 and PLK10. Recombinant PrP aggregate generated in vitro was incubated with 1 μM PLR or PLK and the changes of aggregate levels were monitored by reading ThT fluorescence during the 36 h time course. CTRL, preformed aggregates incubated with no PLR or PLK. **b** Destabilization of PK-resistant PrP^{Sc} of ScN2a cells using PLR38.5 at various pHs. ScN2a cell lysate was incubated with or without PLR at pH 4–7, and the changes of PK-resistant PrP^{Sc} levels were monitored by western blotting. Different glycoforms of PK-resistant PrP^{Sc} were marked with brackets. *D* diglycosylated, *M* monoglycosylated, *U* unglycosylated

Complex formation of plasminogen with PLR occurs more effectively than with PLK

Our previous study demonstrates that inhibition of PrP^{Sc} propagation with PLK is associated with its complex formation with plasminogen [16–18]. Based on the similar polarity of the functional groups in PLR and PLK, binding of PLR with plasminogen was tested using gel electrophoretic migration retardation assay in polyacrylamide gels. Compared to the control, in which plasminogen was incubated with no polymers, migration of PLK33–plasminogen complex was retarded in the gel, while PLR38.5–plasminogen complex was not detected (Fig. 6a). Retarded migration and disappearance of complex bands were dependent on the concentration of polymers incubated with plasminogen. When complexed with plasminogen, PLR10 and PLK10 behaved similarly to corresponding polymers with high molecular weight (Fig. 6b). However, disappearance of the complex band in the gel is less effective, showing the residual band shift of the plasminogen–PLR10 complex at the low concentration of polymers. Protein assay to quantitate

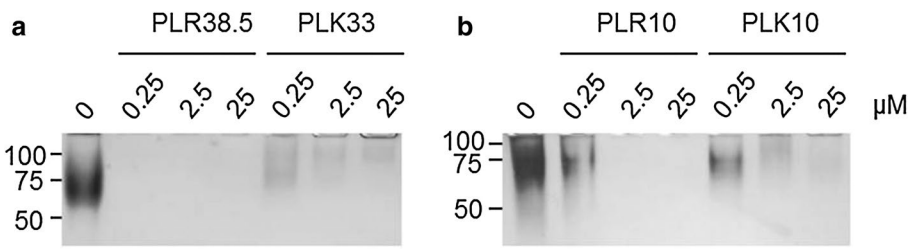

Fig. 6 Comparison of complex formation of plasminogen with PLRs and PLKs. **a** PLR38.5 and PLK33, **b** PLR10 and PLK10. After purified plasminogen (0.25 μM) was incubated with indicated concentrations of PLR and PLK, the polymer–plasminogen complexes were subjected to non-denaturing polyacrylamide gel electrophoresis and stained by silver staining

the amount of proteins in the samples revealed that an absolute level of added proteins remained unchanged after plasminogen and polymers were mixed for complex formation, suggesting no protein degradation of plasminogen by polymers even after the complex was formed. DLS analysis of the generated plasminogen-polymer complex particles demonstrated that PLRs and PLKs form the complexes of various sizes. The average size of the particles was inversely proportional to the molecular weight of polymers used to form the complex with plasminogen (Table 1). Moreover, the sizes of the particles formed with either PLRs or PLKs were not different ($p > 0.05$), suggesting that the ability of both PLRs and PLKs to form a complex with plasminogen is identical. However, further analysis by ELS to measure the zeta potential of the particle demonstrated that the surface charge of the plasminogen–PLR complexes became more positive than that of the plasminogen–PLK complexes, independently of the molecular weights of polymers (Table 1; $p < 0.01$).

Therefore, complete or partial disappearance of the bands representing the plasminogen–polymer complexes (Fig. 6) might be due to the positive surface charges of the complex, by which the complex migrates toward the anode, not entering into the gel. The greater particle size and less positive surface charges of the complex composed of plasminogen and polymers with lower molecular weights propose that disappearance of the complex bands in the gel is not simply explained by the bulkiness of complex which interferes with migration of complex into the gel. Our gel electrophoretic and DLS/ELS results suggest that PLRs produce the complex with plasminogen more effectively than PLKs. These data correlate with the superior anti-prion activity of PLR to PLK.

Discussion

In this study, we report, for the first time, that PLR suppresses the propagation of PrP^{Sc} more effectively than PLK, and the cytotoxicity of PLR and PLK is almost identical. The efficacious concentrations of PLR to inhibit PrP^{Sc} propagation is achieved safely below the cytotoxic concentrations in prion-infected cultured cells. PLR would be more appropriate than PLK as an agent to suppress prions, although in vivo efficacy test results remain to approve the utility of PLR for clinical purpose.

The studies indicate that anti-prion activity of PLR is not due to its cytotoxicity to infected cells, alteration of the PrP^{C} level, degradation of preformed PrP aggregates, or destabilization of PrP^{Sc}. The unchanged PrP^{C} level by PLR suggests that prion inhibition by PLR was not exerted through depleting PrP^{C}, the conformational precursor of PrP^{Sc}. No changes in the states of preformed recombinant PrP aggregates and PrP^{Sc} from prion-infected cells suggest that PrP^{Sc} inhibition by PLR was not mediated through destabilization of pre-existing PrP^{Sc} molecules. Taken together with the results of anti-prion activity of PLR and PLK demonstrated in the current and previous studies [17, 18], it is possible to speculate that PLR inhibits prions by forming complexes with plasminogen, which, in turn, prevents the pathologic role of plasminogen as a cofactor for PrP^{C} conversion to PrP^{Sc}. The functional consequence of PLR–plasminogen complex formation requires to be investigated. Nonetheless, the current study proposes a plausible mechanistic perspective to be determined for the superior anti-prion activity of PLR to PLK. The plasminogen complex with PLR generated more positively charged surface, although PLR and PLK produced the complex of

Table 1 Particle size and zeta potential of the plasminogen–polymer complex

Sample Particle size	Average (nm)	S.D. (nm)	*p* value[a]
Plasminogen	7.3	0.1	
Plasminogen + PLR38.5	140.7	8.2	0.0627
Plasminogen + PLK33	172.5	19.9	
Plasminogen + PLR10	535.9	44.5	0.3927
Plasminogen + PLK10	563.1	21.1	
Sample Zeta potential	Average (mV)	S.D. (mV)	*p* value[a]
Plasminogen	−6.2	0.2	
Plasminogen + PLR38.5	16.0	0.6	0.0003
Plasminogen + PLK33	9.9	0.6	
Plasminogen + PLR10	5.22	0.12	0.0099
Plasminogen + PLK10	4.27	0.34	

[a]Student's *t* test was performed for statistical analysis

comparable sizes. This can be interpreted that PLR binds to plasminogen more effectively than PLK, which raises the possibility of greater ability of PLR in blocking the cofactor function of plasminogen to generate PrP^{Sc} than PLK.

Alternatively, interaction of PLR with PrP^{C} could be associated with anti-prion activity of PLR. Because previous studies [32] reported that anti-prion activity of PLK correlates with its direct binding to PrP^{C}, investigation on the possibility of PLR interaction with PrP^{C} and its relevance to anti-prion activity of PLR is of interest. If this turns out to be the case, together with our findings demonstrated in this study, it is feasible to speculate that there exist multiple molecular events involved in PLR action to suppress prions. It is noteworthy that PLR could exert anti-prion activity through interfering with two independent targets, a cofactor and the PrP^{C} substrate. This may explain why blocking a single cofactor among many other potential cofactors is so efficient to inhibit PrP^{Sc} formation. In fact, there are many other macromolecules known to function as cofactors in propagation of either PrP^{Sc} or prion infectivity. For instance, lipids and polyanions drive a conformational change similar to that occurs during PrP^{C} to PrP^{Sc} conversion [33, 34]. Furthermore, lipids and polyanions (RNA) are critical in acquisition of infectivity for synthetic prions [35, 36]. Concerning the action mechanism of PLR, involvement of lipids or polyanions remains to be investigated, although it is intriguing that interaction of PLR with lipid or polyanions can be easily expected due to their electrostatic properties.

Acknowledgements This research was supported by the grants of the Korea Health Technology R&D Project through the Korea Health Industry Development Institute (KHIDI) funded by the Ministry of Health and Welfare, Republic of Korea (HI16C1085, HI16C0965) and the National Research Foundation of Korea (2012R1A1A2043356).

References

1. Fitch CA, Platzer G, Okon M, Garcia MB, McIntosh LP (2015) Arginine: its pKa value revisited. Protein Sci 24:752–761
2. Oh D et al (2014) Enhanced cellular uptake of short polyarginine peptides through fatty acylation and cyclization. Mol Pharm 11:2845–2854
3. Emi N, Kidoaki S, Yoshikawa K, Saito H (1997) Gene transfer mediated by polyarginine requires a formation of big carrier-complex of DNA aggregate. Biochem Biophys Res Commun 13:231(2):421–424
4. Haider M, Ghandehari H (2003) Influence of poly(amino acid) composition on the complexation of plasmid dna and transfection efficiency. J Bioact Compat Polym 18:293–111
5. Takechi Y et al (2011) Physicochemical mechanism for the enhanced ability of lipid membrane penetration of polyarginine. Langmuir 27:7099–7107
6. Kibler KV et al (2004) Polyarginine inhibits gp160 processing by furin and suppresses productive human immunodeficiency virus type 1 infection. J Biol Chem 279(47):49055–49063
7. Ginsburg I, Borinski R, Malamud D, Struckmeier F, Klimetzek V (1985) Chemiluminescence and superoxide generation by leukocytes stimulated by polyelectrolyte-opsonized bacteria: Role of histones, polyarginine, polylysine, polyhistidine, cytochalasins, and inflammatory exudates as modulators of oxygen burst. Inflammation 9:245–271
8. Heckl S et al (2008) A novel polyarginine containing Smac peptide conjugate that mediates cell death in tumor and healthy cells. Med Chem 4:348–354
9. Rizk SL, Mold C, Haklin M, Roseman DL (1986) The role of C-reactive protein and polyarginine in tumor immunotherapy. Cancer 58:55–61
10. Yang Y, Wolfram J, Fang X, Shen H, Ferrari M (2014) Polyarginine induces an antitumor immune response through binding to toll-like receptor 4. Small 10:1250–1254
11. Prusiner SB (1997) Prion diseases and the BSE crisis. Science 278:245–251
12. Prusiner SB et al (1983) Scrapie prions aggregate to form amyloid-like birefringent rods. Cell 35:349–358
13. Ryou C (2011) Prion diseases. In: Harper D (ed) Encyclopedia of Life Sciences. Wiley, Chichester, pp 1–11
14. Lee J et al (2015) Laboratory diagnosis and surveillance of Creutzfeldt–Jakob disease. J Med Virol 87:175–186
15. Mays CE, Ryou C (2011) Plasminogen: A cellular protein cofactor for PrPSc propagation. Prion 5:22–27
16. Mays CE, Ryou C (2010) Plasminogen stimulates propagation of protease-resistant prion protein in vitro. FASEB J 24:5102–5112
17. Ryou C, Titlow WB, Mays CE, Bae Y, Kim S (2011) The suppression of prion propagation using poly-L-lysine by targeting plasminogen that stimulates prion protein conversion. Biomaterials 32:3141–3149
18. Jackson KS, Yeom J, Han Y, Bae Y, Ryou C (2013) Preference toward a polylysine enantiomer in inhibiting prions. Amino Acids 44:993–1000
19. Wernersson E et al (2010) Effect of association with sulfate on the electrophoretic mobility of polyarginine and polylysine. J Phys Chem B 114:11934–11941
20. Zama M, Ichimura S (1971) Difference between polylysine and polyarginine in changing DNA structure upon complex formation. Biochem Biophys Res Commun 44:936–942
21. Kang HE et al (2012) Characterization of conformation-dependent prion protein epitopes. J Biol Chem 287:37219–37232
22. Kim DH, Lee HM, Ryou C (2014) Evaluation of infective property of recombinant prion protein amyloids in cultured cells overexpressing cellular prion protein. J Korean Med Sci 29:1604–1609
23. Scott MR et al (1988) Prion protein gene expression in cultured cells. Protein Eng 2:69–76
24. Birkett CR et al (2011) Scrapie strains maintain biological phenotypes on propagation in a cell line in culture. EMBO J 20:3351–3358
25. Bian J et al (2010) Cell-based quantification of chronic wasting disease prions. J Virol 84:8322–8326
26. Kim SG, Lee HM, Ryou C (2014) Parameters that affect macromolecular self-assembly of prion protein. Protein J 33:243–252
27. Lim YB, Mays CE, Kim Y, Titlow WB, Ryou C (2010) The inhibition of prions through blocking prion conversion by permanently charged branched polyamines of low cytotoxicity. Biomaterials 31:2025–2033
28. Wessel D, Flügge UI (1984) A method for the quantitative recovery of protein in dilute solution in the presence of detergents and lipids. Anal Biochem 138:141–143
29. Doorley GW, Payne CK (2011) Cellular binding of nanoparticles in the presence of serum proteins. Chem Commun 47:466–468
30. Supattapone S et al (2001) Branched polyamines cure prion-infected neuroblastoma cells. J Virol 75:3453–3346

31. McCarthy JM et al (2013) Influence of surface groups on poly(propylene imine) dendrimers antiprion activity. Biomacromolecules 14:27–37
32. Xu Z et al (2011) Mechanistic insights into cellular alteration of prion by poly-D-lysine: the role of H2H3 domain. FASEB J 25:3426–3435
33. Wong C et al (2001) Sulfated glycans and elevated temperature stimulate PrP(Sc)-dependent cell-free formation of protease-resistant prion protein. Embo J 20: 377–386.
34. Wang F et al (2007) Lipid interaction converts prion protein to a PrPSc-like proteinase K-resistant conformation under physiological conditions. Biochemistry 46:7045–7053
35. Deleault NR, Lucassen RW, Supattapone S (2003) RNA molecules stimulate prion protein conversion. Nature 425:717–720
36. Deleault NR et al (2012) Isolation of phosphatidylethanolamine as a solitary cofactor for prion formation in the absence of nucleic acids. Proc Natl Acad Sci USA 109:8546–8551